Airway antibodies wane rapidly after COVID-19 but B cell memory is generated across disease severity

Alberto Cagigi[1], Meng Yu[1], Sara Falck-Jones[1], Sindhu Vangeti[1], Björn Österberg[1], Eric Åhlberg[1], Lida Azizmohammadi[1], Ryan Falck-Jones[2,3], Pia C Gubisch[1], Mert Ödemis[1], Farangies Ghafoor[1], Klara Lenart[1], Max Bell[2,3], Niclas Johansson[4,5], Jan Albert[6,7], Jörgen Sälde[8], Deleah Pettie[9,10], Michael Murphy[9,10], Lauren Carter[9,10], Neil P King[9,10], Sebastian Ols[1], Anna Färnert[4,5], Karin Loré[1*] and Anna Smed-Sörensen[1*]

[1]Division of Immunology and Allergy, Department of Medicine Solna, Karolinska Institutet, Karolinska University Hospital, Stockholm, Sweden. [2]Department of Physiology and Pharmacology, Karolinska Institutet, Stockholm, Sweden. [3]Department of Perioperative Medicine and Intensive Care, Karolinska University Hospital, Stockholm, Sweden. [4]Division of Infectious Diseases, Department of Medicine Solna, Center for Molecular Medicine, Karolinska Institutet, Sweden. [5]Department of Infectious Diseases, Karolinska University Hospital Solna, Stockholm, Sweden. [6]Department of Microbiology, Tumor and Cell Biology, Karolinska Institutet, Stockholm, Sweden. [7]Clinical Microbiology, Karolinska University Hospital Solna, Stockholm, Sweden. [8]Närakut SLSO, Karolinska University Hospital Solna, Stockholm, Sweden. [9]Department of Biochemistry, University of Washington, Seattle, WA 98195, United States. [10]Institute for Protein Design, University of Washington, Seattle, WA 98195, United States. [*]Equal contribution.

Correspondence to:
Karin Loré and Anna Smed-Sörensen, Division of Immunology and Allergy, Department of Medicine Solna, Karolinska Institutet, Visionsgatan 4, BioClinicum J7:30, Karolinska University Hospital, 171 64 Stockholm, Sweden.
e-mail addresses: karin.lore@ki.se; anna.smed.sorensen@ki.se

Conflict of interest statement
The authors have declared that no conflict of interest exists.

Summary

COVID-19 severity determines the level of systemic and airway IgG and IgA but while IgG are maintained in plasma during convalescence, antibodies wane rapidly in the airways. However, comparable levels of antigen-specific memory B cells are generated across disease severity.

Abstract

Understanding immune responses following SARS-CoV-2 infection in relation to COVID-19 severity is critical for predicting the effects of long-term immunological memory on viral spread. Here we longitudinally assessed systemic and airway immune responses against SARS-CoV-2 in a well-characterized cohort of 147 infected individuals representing the full spectrum of COVID-19 severity; from asymptomatic infection to fatal disease. High systemic and airway antibody responses were elicited in patients with moderate to severe disease, and while systemic IgG levels were maintained after acute disease, airway IgG and IgA declined significantly. In contrast, individuals with mild symptoms showed significantly lower antibody responses but their levels of antigen-specific memory B cells were comparable with those observed in patients with moderate to severe disease. This suggests that antibodies in the airways may not be maintained at levels that prevent local virus entry upon re-exposure and therefore protection via activation of the memory B cell pool is critical.

Introduction

Severe acute respiratory syndrome coronavirus 2 (SARS-CoV-2) infection that causes coronavirus disease 2019 (COVID-19) can present with a wide range of disease severity from asymptomatic to fatal. Individuals of advanced age and/or those with comorbidities are overrepresented among patients who develop severe disease (Zaki et al., 2020). However, the majority of SARS-CoV-2 infected individuals experience asymptomatic infection or only mild disease (Moghadas et al., 2020). Understanding immune responses following SARS-CoV-2 infection in relation to COVID-19 severity is critical for predicting long-term immunological memory and the potential risk for re-infection or virus spread. Whether patients with different disease severities generate similar protective immunity is still unknown. Here we present longitudinal data on virus-specific systemic and airway antibody and B cell memory responses generated in a clinically well-characterized cohort of individuals with SARS-CoV-2 infection (n=147) representing the full spectrum of COVID-19 severity ranging from asymptomatic infection to fatal disease.

Results and discussion

Individuals were sampled during disease and convalescence with longitudinal, donor-matched blood and airway samples. The levels of systemic and airway antibody responses as well as the generation of SARS-CoV-2-specific memory B cells were measured. Plasma, peripheral blood mononuclear cells (PBMC), nostril swabs (NSW) and nasopharyngeal aspirates (NPA) were collected across all disease severities whereas endotracheal aspirates (ETA) were collected only from intubated patients receiving intensive care (Figure 1A). Disease severity was assessed daily, using a seven-point scale derived from the respiratory domain of the sequential organ failure assessment (SOFA) score (Grissom et al., 2010; Vincent et al., 1996), with additional levels for non-admitted mild cases (1) and fatal cases (7). Patients were later grouped based on peak disease severity (PDS) (Table 1). In addition, pre-pandemic healthy controls (PPHC) (n=30) as well as individuals who experienced influenza-like symptoms and were possibly exposed to SARS-Cov-2 but had a negative diagnostic PCR (PCR-) (n=9) were sampled in the same way and included as controls.

We first assessed systemic IgG and IgA responses at the time of study inclusion that ranged between 0-54 days from onset of symptoms; median 16 days. Generally, patients with the highest peak disease severity score were included in the study after they had already been hospitalized for a number of days (Figure 1B) (Falck-Jones et al., 2020). Therefore, these individuals were sampled longer after symptom onset as compared with individuals with mild disease resulting in a large time frame of study inclusion with respect to symptom onset (Table 1). For simplicity, this sampling period/study inclusion is referred to as the “acute” phase. Samples collected at the first follow-up visit (46-168 days; median 108 days) are referred to as the “convalescent” phase. Time of convalescent from acute sampling ranged based on individual patient recovery and their disease severity (33-159 days; median 90 days). Plasma IgG and IgA against the SARS-CoV-2 nucleocapsid (N) and spike (S) proteins as well as the receptor binding domain (RBD) (Walls et al., 2020; Wrapp et al., 2020) of the S protein were measured by ELISA. Antibody responses against the internal N protein have been shown to be elevated in deceased individuals but whether these antibodies contribute

103 to disease severity is unknown (Atyeo et al., 2020; Guthmiller et al., 2020). In contrast,
104 antibody responses against the viral surface protein S and, in particular, against the RBD
105 result in virus neutralization (Piccoli et al., 2020). Responses against the RBD are thus likely
106 necessary for protection from re-infection or prevention of symptomatic disease.
107
108 In line with previous reports (Atyeo et al., 2020; Gaebler et al., 2020; Gudbjartsson et al.,
109 2020; Guthmiller et al., 2020; Zhao et al., 2020), plasma IgG and IgA responses against N, S
110 and RBD were robust in acute disease in the majority of individuals with moderate to severe
111 disease while they were substantially lower in individuals with mild disease (Figure 2A).
112 However, in our cohort, this might also partially be due to earlier study inclusion of patients
113 with mild symptoms (median days from onset of symptoms 11 as compared with 13 and
114 21.5 in the moderate and severe groups respectively, and 13 in the fatal group) (Table 1). In
115 fact, while plasma IgG levels remained high in the patients with moderate to severe disease
116 in the convalescent phase, levels had increased in the individuals with mild disease and all
117 had seroconverted (Figure 2A). In contrast, IgA levels from the acute phase, against all
118 antigens, waned substantially during convalescence in most patients (Figure 2A). While the
119 levels of IgG against the RBD (Figure 2B), as well as against N and S (Figure S1A), exhibited a
120 positive correlation with days from onset of symptoms during the acute phase, this was less
121 pronounced for IgA levels. Furthermore, patients with mild disease displayed lower levels of
122 plasma IgG against RBD as compared with more severe patients, also when samples were
123 taken after similar duration of symptoms (Figure 2A-B and Figure S1B). Altogether, these
124 data confirm that the generation of IgA likely precede that of IgG. Earlier reports of
125 individuals with asymptomatic infection or mild disease also showed robust early IgA
126 responses (Cervia et al., 2020; Staines et al., 2020; Sterlin et al., 2020).
127
128 Comparable to another study (Hansen et al., 2020), the levels of both plasma IgG and IgA
129 against all antigens tested, during both acute disease and convalescence, were significantly
130 higher in patients with more severe disease compared to mild, both when comparing
131 disease severity at time of study inclusion and initial sampling as well as when grouping the
132 patients based on their peak disease severity (Figure S2A). When comparing antibody levels
133 between disease severity groups based on when patients were sampled after disease onset,
134 patients with moderate or severe disease on average tended to have higher antibodies
135 compared to those with mild disease already during the first week of symptom onset and
136 were more pronounced after 2, 3 and >3 weeks of symptom onset (Figure S1B). However,
137 these differences were not statistically significant in our cohort, probably due to uneven
138 inclusion over time in the different disease severity groups. In our cohort, the difference in
139 antibody titers over time was further supported by the fact that the patients with
140 moderate/severe disease, and even fatal outcome, for whom we initially observed low IgG
141 titers against RBD, had an early study inclusion (on average 13 days from onset of
142 symptoms); but showed significantly higher titers later during the acute phase (on average
143 19 days) (Figure 2C-D). Similar kinetics of anti-RBD responses have previously been noted in
144 different patient cohorts (Lynch et al., 2020; Robbiani et al., 2020; Rydyznski Moderbacher
145 et al., 2020).
146
147 As the respiratory tract is the initial site of viral infection and replication, we next measured
148 the levels of IgG and IgA in the upper and lower airways and compared with levels in plasma
149 at matched time points. Due to limited sample volumes, we focused our analyses on IgG and

150 IgA responses against the RBD since these responses are likely most critical for virus
151 neutralization. We found that RBD-specific antibodies could be readily detected in NSW and
152 NPA during the acute phase in several patients across all disease severities (Figure 3A and B).
153 In agreement with our observations in plasma, antibody levels in the upper respiratory tract
154 were higher in patients with moderate or severe disease as compared with individuals with
155 mild disease. Both IgG and IgA levels declined significantly in the convalescent phase, with
156 IgG declining to almost undetectable levels (Figure 3A and B). This demonstrates that airway
157 antibody levels wane much faster than those in plasma during convalescence. Low but
158 detectable levels of antibodies to SARS-CoV-2 have previously been reported also in saliva
159 during convalescence (Isho et al., 2020). However, whether these low antibody levels at
160 mucosal sites will be sufficient for protection is not known. We found that RBD-specific IgG
161 and IgA levels in the respiratory tract correlated well with those in plasma during the acute
162 phase but to a lesser extent during convalescence (Figure 3C and Figure S2B). When
163 comparing donor-matched NSW, NPA and ETA collected at the same time point during acute
164 disease from intubated patients, significantly higher levels of IgA against the RBD were found
165 in NPA as compared with NSW and ETA (Figure 3D). While this could be partially influenced
166 by differences in sampling method and sample volume, these data suggest that antibody
167 abundance and possibly virus neutralization via IgA differs along the respiratory tract and
168 may be more pronounced in the nasopharynx compared to the lower airways. Hence,
169 nasopharynx antibodies (both IgG and IgA) showed a strong correlation with plasma
170 antibody responses (Figure 3D and Figure S2B). We also assessed the presence of B cells in
171 the respiratory tract of COVID-19 patients by analyzing the lymphocytes that could be
172 retrieved from NPA and ETA as compared with NPA from three additional healthy controls
173 (HC). Lymphocyte frequencies were lower in both NPA and ETA from several COVID-19
174 patients as compared with NPA from HC. The proportion of B cells of lymphocytes was
175 similar in NPA from HC and COVID-19 patients. However, the proportion of B cells in ETA of
176 COVID-19 patients was lower compared to NPA, which possibly contributes to the higher
177 antibody levels at this site (Figure 4A and B).
178
179 Altogether, the data presented so far confirm that moderate and severe COVID-19 result in
180 high levels of circulating antibodies and show that despite IgG being well-maintained during
181 convalescence, antibody levels in the airways decline significantly after the acute phase.
182 Generally, antibodies present in circulation and at local sites are the result of secretion from
183 short-lived plasmablasts and/or terminally differentiated plasma cells in the bone marrow or
184 mucosal sites (Zielinski et al., 2011). The response to a secondary infection once antibody
185 titers have waned below protective levels mostly relies on the presence of resting antigen-
186 specific memory B cells that are rapidly activated upon antigen re-exposure (Zielinski et al.,
187 2011). We therefore investigated the induction and maintenance of antigen-specific
188 memory B cells similar to other studies (Dan et al., 2020; Juno et al., 2020; Rodda et al.,
189 2020). We focused on the direct comparison between individuals with mild disease and
190 patients with moderate/severe disease, along with individuals who had reported mild
191 influenza-like symptoms but were SARS-CoV-2 PCR-. Patients with moderate/severe disease
192 who had high circulating IgG and IgA levels were specifically selected for the analysis to be
193 able to compare the opposite ends of the COVID-19 disease spectrum. Donor-matched
194 PBMC from acute disease and convalescence were analyzed side-by-side using fluorescently
195 labelled S and RBD probes to detect antigen-specific B cells (Dan et al., 2020; Juno et al.,
196 2020; Rodda et al., 2020). Patients with moderate/severe disease had switched memory B

197 cells specific to S in the acute phase and the memory B cell pool had further expanded in the
198 convalescent phase (ranging from 0.009 to 1.35%; mean 0.42% during convalescence)
199 (Figure 4C-F). Individuals with mild disease showed lower memory B cells during acute
200 disease than the patients with moderate/severe disease, but the levels had increased by the
201 time of convalescent sampling (ranging from 0.17% to 0.64%; mean 0.35% during
202 convalescence) and were comparable between the groups (Figure 4E and F). Further
203 phenotyping of the S-specific memory B cells indicated that the majority of these cells may
204 be specific for epitopes on S outside of the RBD (Figure 4D). However, it is possible that
205 binding of B cells to RBD could be underestimated as RBD is also present in the S protein. S-
206 specific memory B cells in the circulation were predominantly IgG+, rather than IgA+ (Figure
207 4D). Low frequencies of S and RBD-specific memory B cells were observed in the PCR-
208 individuals. However, these were not significantly different from the levels observed in PPHC
209 (Figure 4C and E). Collectively, since the majority of individuals infected with SARS-CoV-2 are
210 either asymptomatic or experience only mild COVID-19 symptoms (Moghadas et al., 2020),
211 the possibility of generating antigen-specific memory B cells without experiencing severe
212 disease, would be very important in the prospect of establishing potential immunity at the
213 population level.
214
215 In summary, here we show that COVID-19 disease severity not only determines the
216 magnitude of systemic but also airway antibody levels with efficient generation of virus-
217 specific memory B cells against SARS-CoV-2 also occurring upon mild disease. While plasma
218 IgG levels were generally well detectable at convalescence in all groups, there was a
219 significant decline in airway antibodies after the clearance of infection. This suggests that
220 antibodies in the airways may not be maintained at levels that prevent local virus entry upon
221 re-exposure. However, our data indicate that the majority of infected individuals have the
222 ability to generate anamnestic responses via the memory B cell pool. Speculatively, the
223 antibodies and memory B cell pool may play a role for protection or mitigation of disease
224 severity in case of re-infection. Whether sufficient number of memory B cells will be
225 maintained long-term and to what extent they will prevent the spread of SARS-CoV-2 at the
226 population level remain to be understood. This is critical knowledge to acquire in the near
227 future to evaluate together with the memory B cell response generated after the
228 introduction of SARS-CoV-2 vaccination. Ultimately, the requirements for establishment of
229 long-term protection and immunity will need to be determined.
230
231
232 **Materials and methods**
233
234 **Study design, patient enrollment and sample collection**
235 One hundred and forty-seven (147) PCR-confirmed SARS-CoV-2 infected patients were
236 enrolled at the Karolinska University Hospital and Haga Outpatient Clinic (Haga Närakut),
237 Stockholm, Sweden during March-May 2020 (acute phase) in a time that ranged from 0 to
238 54 days from onset of symptoms as self-reported by individual patients; and during April-
239 September 2020 (convalescence) in a time that ranged from 46 to 168 days continuing from
240 the previous counts. Patients were enrolled at various settings, ranging from primary to
241 intensive care. In order to recruit asymptomatic and mild cases, household contacts of
242 COVID-19 patients were screened with PCR and enrolled if positive. A small subset of these
243 individuals who experienced influenza-like symptoms and were possibly exposed to SARS-

Cov-2 but had a negative diagnostic PCR (PCR-) (n=9 of whom 3 were household contacts of confirmed patients with 1 experiencing fever, and 6 were included based on suspected infection with 4 experiencing fever) were sampled in the same way and included as controls alongside with 30 pre-pandemic healthy control samples (PPHC) from 2016-2018.

Respiratory failure was categorized daily according to the respiratory domain of the Sequential Organ Failure Assessment score (SOFA)(Vincent et al., 1996). The modified SOFA score (mSOFA) was calculated when arterial partial pressure of oxygen (PaO_2) was not available. In this case peripheral transcutaneous hemoglobin saturation (SpO_2) was used instead (Grissom et al., 2010). Estimation of the fraction of inspired oxygen (FiO_2) based on O_2 flow was calculated as per the Swedish Intensive Care register definition (Intensivvårdsregistret, 2018). Patients were categorized based on the peak respiratory SOFA or mSOFA value with the 5-point respiratory SOFA score being extended with additional levels to include and distinguish admitted asymptomatic and non-admitted/admitted mild cases and to include fatal outcome added as a seventh level. Ten (10) patients with fatal outcome had peak disease severity score 6 prior to death and 2 patients had scores of 4 and 5. For convenience, the resulting 7-point composite peak disease severity (PDS) was condensed into a broader classification consisting of mild (1-2), moderate (3-4), severe (5-6), and fatal (7). Demographics and additional data were collected from medical records, including clinical history and risk factors such as BMI and co-morbidities. Total burden of comorbidities was assessed using the Charlson co-morbidity index (CCI) (Charlson et al., 1987) (Table 1). Additional clinical information on this patient cohort including the modulation of disease from time to study inclusion to peak severity can be found in Falck-Jones et al (Falck-Jones et al., 2020).

Blood was collected in EDTA-containing tubes from all patients except those admitted to the intensive care unit (ICU) for whom blood was pooled from heparin-coated blood gas syringes discarded in the last 12 hours. For some ICU patients, additional venous blood was also collected in EDTA tubes. Nostril swabs (NSW) and nasopharyngeal aspirates (NPA) were collected from the majority of the patients whereas endotracheal aspirates (ETA) were only collected from patients with mechanical ventilation intubated in the ICU. Admitted patients were sampled during acute disease at up to four timepoints and ICU patient material was collected up at to ten timepoints. For this study, unless otherwise stated, the measurements referring to acute disease were performed with samples collected at the time of study inclusion and during convalescence when patients returned for a follow-up visit.

The study was approved by the Swedish Ethical Review Authority, and performed according to the Declaration of Helsinki. Written informed consent was obtained from all patients and controls. For sedated patients, the denoted primary contact was contacted and asked about the presumed will of the patient and to give initial oral and subsequently signed written consent. When applicable retrospective written consent was obtained from patients with non-fatal outcomes.

Enzyme-linked immunosorbent assay (ELISA)

The presence of IgG or IgA binding against the SARS-Cov-2 Nucleocapsid (N) and Spike (S) trimer or the Receptor Binding Domain (RBD) monomer (Walls et al., 2020) in plasma and airway samples was assessed by enzyme-linked immunosorbent assay (ELISA). Recombinant

291 proteins were received through the global health-vaccine accelerator platforms (GH-VAP)
292 funded by the Bill & Melinda Gates Foundation. Briefly, 96-half well plates were coated with
293 50ng/well of the respective protein. Plates were incubated with a selected duplicate dilution
294 that did not provide background noise against ovalbumin used as a negative control (data
295 not shown) (i.e. 1:20 for plasma samples, 1:2 for NSW and NPA, and 1:5 for ETA in 5%
296 milk/PBS buffer). Duplicate 7-point serial dilutions were initially performed for measuring
297 plasma IgG against RBD during acute disease and the half maximal effective concentration
298 (EC_{50}) was calculated using GraphPad Prism 9. However, since for several samples with low
299 antibody concentration (mostly from the asymptomatic/mild category) the EC_{50} was below
300 the highest dilution used (of 1:20) and therefore below the limit of detection (Figure S3A),
301 the maximal optical density (OD) at 1:20 dilution was used instead for this and for all the
302 other measurements subsequently performed. The relation with maximal OD and EC_{50} was
303 also verified in a subset of patients with high IgG and IgA against S (Figure S3B). Detection
304 was performed with mouse and goat anti-human IgG or IgA HRP-conjugated secondary
305 antibodies (clone G18-145 from BD Biosciences and polyclonal from ThermoFisher,
306 respectively) followed by incubation with TMB substrate (BioLegend) which was stopped
307 with a 1M solution of sulfuric acid. Blocking with 5% milk/PBS buffer and washing with 0.1%
308 Tween-20/PBS buffer were performed between each step. Absorbance was read at 450nm
309 and background correction at 550nm using an ELISA reader. Data were reported as maximal
310 absorbance i.e. OD, as stated above, and plotted using GraphPad Prism 9. All of the antibody
311 measurements in plasma and respiratory samples from SARS-CoV-2 patients were run
312 alongside with samples from two different control groups as described above. Interestingly,
313 low but readily detectable IgA reactivity against S was detected in the pre-pandemic healthy
314 controls and in the PCR- individuals (Figure S3C). After having verified the specificity and
315 sensitivity of our ELISA assay for IgA detection with limiting sample dilutions (Figure S3D), we
316 hypothesize that this might be due to cross-reactivity on the shared portions of the S protein
317 between SARS-CoV-2 and other common cold coronaviruses. Reports have shown that cross-
318 reactivity between coronaviruses exists (Grifoni et al., 2020; Song et al., 2020).
319
320 **Flow cytometry**
321 Staining of cells from airway samples was performed fresh. Briefly, samples were centrifuged
322 at 400 g for 5 min at room temperature and cells were washed with sterile PBS. Mucus was
323 removed using a 70 μm cell strainer and cells were subsequently stained with the
324 appropriate combination of fluorescently labelled monoclonal antibodies as illustrated in
325 Figure 4A. Staining of PBMC was performed on previously cryopreserved samples. The
326 appropriate combination of fluorescently labelled monoclonal antibodies binding to
327 different cell surface markers and with fluorescently labelled S and RBD proteins used as
328 probes for antigen-specific B cells is illustrated in Figure 4C. Probes were prepared from
329 biotinylated proteins using a 4:1 molar ratio (protein:fluorochrome-labelled streptavidin)
330 considering the molecular weight of protein monomers and of the streptavidin only. The
331 probes were prepared using streptavidin conjugated to PE and APC for S and with BV421 for
332 the RBD. The gating strategy for the identification of antigen-specific memory B cells is
333 shown in Figure 2d. Briefly, after identification of lymphocytes in single suspension, live B
334 cells, (i.e. cells not expressing CD3/,CD14/CD16/CD56) were gated. From this gate, B cells
335 were further isolated by expression of CD19 and CD20 and then switched memory B cells
336 were identified as IgD-IgM-. From these, S-specific switched memory B cells were identified
337 by binding to both S protein probes. Further characterization was then carried out by

analyzing IgG expression (IgA+ switched memory B cells are assumed to mirror IgD-IgM-IgG-B cells) and fluorescently labelled RBD. Stained cells from airway samples were acquired using a BD LSRFortessa while stained PBMC were acquired using a BD FACSAria Fusion both interfaced with the BD FACSDiva Software. Results were analyzed using BD FlowJo version 10.

Statistical analyses

All statistical analyses were performed using GraphPad Prism 9. Spearman correlation was used to assess the interdependence of 2 different non-categorical parameters across individuals whereas Wilcoxon matched-pairs signed rank or Mann–Whitney U tests as appropriate, were used to assess differences or similarities for one single parameter between 2 different groups. Kruskal -Wallis with Dunn's multiple comparisons test was used when assessing comparison between multiple groups.

Author contributions

Experimental study design: A.C., Ka.L. and A.S-S. Clinical concept design: A.S-S., M.B., N.J., J.A., J.S. and A.F. Acquisition and sample processing: M.Y., S. F-J., S.V., B.Ö., E.Å., L.A., R.F-J., M.Ö. and F.G. Generation of data: A.C., M.Y., S. F-J., S.V. and P.C.G. Provision of custom reagents: D.P., M.M., L.C., and N.P.K. Analysis and interpretation of data: A.C., Ka.L. and A.S-S. Critical revision of the manuscript: all authors. Statistical analysis: A.C., K.L. and S.O. Ka.L. and A.S-S. contributed equally to the study.

Acknowledgments

We thank the patients and healthy volunteers who have contributed to this study. We would also like to thank medical students and hospital staff for assistance with patient sampling and collection of clinical data, the Biomedicum BSL3 core facility, Karolinska Institutet and Fredrika Hellgren for assistance with English editing. This work was supported by grants from the Swedish Research Council, the Swedish Heart-Lung Foundation, the Bill & Melinda Gates Foundation, the Knut and Alice Wallenberg Foundation through SciLifeLab and Karolinska Institutet.

372 **References**
373
374 Atyeo, C., S. Fischinger, T. Zohar, M.D. Slein, J. Burke, C. Loos, D.J. McCulloch, K.L. Newman,
375 C. Wolf, J. Yu, K. Shuey, J. Feldman, B.M. Hauser, T. Caradonna, A.G. Schmidt, T.J.
376 Suscovich, C. Linde, Y. Cai, D. Barouch, E.T. Ryan, R.C. Charles, D. Lauffenburger, H.
377 Chu, and G. Alter. 2020. Distinct Early Serological Signatures Track with SARS-CoV-2
378 Survival. *Immunity* 53:524-532 e524.
379 Cervia, C., J. Nilsson, Y. Zurbuchen, A. Valaperti, J. Schreiner, A. Wolfensberger, M.E. Raeber,
380 S. Adamo, M. Emmenegger, S. Hasler, P.P. Bosshard, E.D. Cecco, E. Bächli, A. Rudiger,
381 M. Stüssi-Helbling, L.C. Huber, A.S. Zinkernagel, D.J. Schaer, A. Aguzzi, U. Held, E.
382 Probst-Müller, S.K. Rampini, and O. Boyman. 2020. Systemic and mucosal antibody
383 secretion specific to SARS-CoV-2 during mild versus severe COVID-19. *bioRxiv*
384 2020.2005.2021.108308.
385 Charlson, M.E., P. Pompei, K.L. Ales, and C.R. MacKenzie. 1987. A new method of classifying
386 prognostic comorbidity in longitudinal studies: development and validation. *J Chronic*
387 *Dis* 40:373-383.
388 Dan, J.M., J. Mateus, Y. Kato, K.M. Hastie, C.E. Faliti, S.I. Ramirez, A. Frazier, E.D. Yu, A.
389 Grifoni, S.A. Rawlings, B. Peters, F. Krammer, V. Simon, E.O. Saphire, D.M. Smith, D.
390 Weiskopf, A. Sette, and S. Crotty. 2020. Immunological memory to SARS-CoV-2
391 assessed for greater than six months after infection. *bioRxiv* 2020.2011.2015.383323.
392 Falck-Jones, S., S. Vangeti, M. Yu, R. Falck-Jones, A. Cagigi, I. Badolati, B. Osterberg, M.J.
393 Lautenbach, E. Ahlberg, A. Lin, I. Szurgot, K. Lenart, F. Hellgren, J. Salde, J. Albert, N.
394 Johansson, M. Bell, K. Lore, A. Farnert, and A. Smed-Sorensen. 2020. Functional
395 myeloid-derived suppressor cells expand in blood but not airways of COVID-19
396 patients and predict disease severity. *medRxiv*
397 Gaebler, C., Z. Wang, J.C.C. Lorenzi, F. Muecksch, S. Finkin, M. Tokuyama, M. Ladinsky, A.
398 Cho, M. Jankovic, D. Schaefer-Babajew, T.Y. Oliveira, M. Cipolla, C. Viant, C.O. Barnes,
399 A. Hurley, M. Turroja, K. Gordon, K.G. Millard, V. Ramos, F. Schmidt, Y. Weisblum, D.
400 Jha, M. Tankelevich, J. Yee, I. Shimeliovich, D.F. Robbiani, Z. Zhao, A. Gazumyan, T.
401 Hatziioannou, P.J. Bjorkman, S. Mehandru, P.D. Bieniasz, M. Caskey, and M.C.
402 Nussenzweig. 2020. Evolution of Antibody Immunity to SARS-CoV-2. *bioRxiv*
403 Grifoni, A., D. Weiskopf, S.I. Ramirez, J. Mateus, J.M. Dan, C.R. Moderbacher, S.A. Rawlings,
404 A. Sutherland, L. Premkumar, R.S. Jadi, D. Marrama, A.M. de Silva, A. Frazier, A.F.
405 Carlin, J.A. Greenbaum, B. Peters, F. Krammer, D.M. Smith, S. Crotty, and A. Sette.
406 2020. Targets of T Cell Responses to SARS-CoV-2 Coronavirus in Humans with COVID-
407 19 Disease and Unexposed Individuals. *Cell* 181:1489-1501 e1415.
408 Grissom, C.K., S.M. Brown, K.G. Kuttler, J.P. Boltax, J. Jones, A.R. Jephson, and J.F. Orme, Jr.
409 2010. A modified sequential organ failure assessment score for critical care triage.
410 *Disaster Med Public Health Prep* 4:277-284.
411 Gudbjartsson, D.F., G.L. Norddahl, P. Melsted, K. Gunnarsdottir, H. Holm, E. Eythorsson, A.O.
412 Arnthorsson, D. Helgason, K. Bjarnadottir, R.F. Ingvarsson, B. Thorsteinsdottir, S.
413 Kristjansdottir, K. Birgisdottir, A.M. Kristinsdottir, M.I. Sigurdsson, G.A. Arnadottir,
414 E.V. Ivarsdottir, M. Andresdottir, F. Jonsson, A.B. Agustsdottir, J. Berglund, B.
415 Eiriksdottir, R. Fridriksdottir, E.E. Gardarsdottir, M. Gottfredsson, O.S. Gretarsdottir,
416 S. Gudmundsdottir, K.R. Gudmundsson, T.R. Gunnarsdottir, A. Gylfason, A. Helgason,
417 B.O. Jensson, A. Jonasdottir, H. Jonsson, T. Kristjansson, K.G. Kristinsson, D.N.
418 Magnusdottir, O.T. Magnusson, L.B. Olafsdottir, S. Rognvaldsson, L. le Roux, G.

419 Sigmundsdottir, A. Sigurdsson, G. Sveinbjornsson, K.E. Sveinsdottir, M. Sveinsdottir,
420 E.A. Thorarensen, B. Thorbjornsson, M. Thordardottir, J. Saemundsdottir, S.H.
421 Kristjansson, K.S. Josefsdottir, G. Masson, G. Georgsson, M. Kristjansson, A. Moller, R.
422 Palsson, T. Gudnason, U. Thorsteinsdottir, I. Jonsdottir, P. Sulem, and K. Stefansson.
423 2020. Humoral Immune Response to SARS-CoV-2 in Iceland. *N Engl J Med* 383:1724-
424 1734.
425 Guthmiller, J.J., O. Stovicek, J. Wang, S. Changrob, L. Li, P. Halfmann, N.Y. Zheng, H. Utset,
426 C.T. Stamper, H.L. Dugan, W.D. Miller, M. Huang, Y.N. Dai, C.A. Nelson, P.D. Hall, M.
427 Jansen, K. Shanmugarajah, J.S. Donington, F. Krammer, D. Fremont, A. Joachimiak, Y.
428 Kawaoka, V. Tesic, M.L. Madariaga, and P.C. Wilson. 2020. SARS-CoV-2 infection
429 severity is linked to superior humoral immunity against the spike. *bioRxiv*
430 Hansen, C.B., I. Jarlhelt, L. Perez-Alos, L. Hummelshoj Landsy, M. Loftager, A. Rosbjerg, C.
431 Helgstrand, J.R. Bjelke, T. Egebjerg, J.G. Jardine, C. Svaerke Jorgensen, K. Iversen, R.
432 Bayarri-Olmos, P. Garred, and M.O. Skjoedt. 2020. SARS-CoV-2 Antibody Responses
433 Are Correlated to Disease Severity in COVID-19 Convalescent Individuals. *J Immunol*
434 Intensivvårdsregistret, S. 2018. SIR:s riktlinje för registrering av SOFA. . In.
435 Isho, B., K.T. Abe, M. Zuo, A.J. Jamal, B. Rathod, J.H. Wang, Z. Li, G. Chao, O.L. Rojas, Y.M.
436 Bang, A. Pu, N. Christie-Holmes, C. Gervais, D. Ceccarelli, P. Samavarchi-Tehrani, F.
437 Guvenc, P. Budylowski, A. Li, A. Paterson, F.Y. Yue, L.M. Marin, L. Caldwell, J.L. Wrana,
438 K. Colwill, F. Sicheri, S. Mubareka, S.D. Gray-Owen, S.J. Drews, W.L. Siqueira, M.
439 Barrios-Rodiles, M. Ostrowski, J.M. Rini, Y. Durocher, A.J. McGeer, J.L. Gommerman,
440 and A.C. Gingras. 2020. Persistence of serum and saliva antibody responses to SARS-
441 CoV-2 spike antigens in COVID-19 patients. *Sci Immunol* 5:
442 Juno, J.A., H.X. Tan, W.S. Lee, A. Reynaldi, H.G. Kelly, K. Wragg, R. Esterbauer, H.E. Kent, C.J.
443 Batten, F.L. Mordant, N.A. Gherardin, P. Pymm, M.H. Dietrich, N.E. Scott, W.H. Tham,
444 D.I. Godfrey, K. Subbarao, M.P. Davenport, S.J. Kent, and A.K. Wheatley. 2020.
445 Humoral and circulating follicular helper T cell responses in recovered patients with
446 COVID-19. *Nat Med*
447 Lynch, K.L., J.D. Whitman, N.P. Lacanienta, E.W. Beckerdite, S.A. Kastner, B.R. Shy, G.M.
448 Goldgof, A.G. Levine, S.P. Bapat, S.L. Stramer, J.H. Esensten, A.W. Hightower, C. Bern,
449 and A.H.B. Wu. 2020. Magnitude and kinetics of anti-SARS-CoV-2 antibody responses
450 and their relationship to disease severity. *Clin Infect Dis*
451 Moghadas, S.M., M.C. Fitzpatrick, P. Sah, A. Pandey, A. Shoukat, B.H. Singer, and A.P.
452 Galvani. 2020. The implications of silent transmission for the control of COVID-19
453 outbreaks. *Proc Natl Acad Sci U S A*
454 Piccoli, L., Y.J. Park, M.A. Tortorici, N. Czudnochowski, A.C. Walls, M. Beltramello, C. Silacci-
455 Fregni, D. Pinto, L.E. Rosen, J.E. Bowen, O.J. Acton, S. Jaconi, B. Guarino, A. Minola, F.
456 Zatta, N. Sprugasci, J. Bassi, A. Peter, A. De Marco, J.C. Nix, F. Mele, S. Jovic, B.F.
457 Rodriguez, S.V. Gupta, F. Jin, G. Piumatti, G. Lo Presti, A.F. Pellanda, M. Biggiogero,
458 M. Tarkowski, M.S. Pizzuto, E. Cameroni, C. Havenar-Daughton, M. Smithey, D. Hong,
459 V. Lepori, E. Albanese, A. Ceschi, E. Bernasconi, L. Elzi, P. Ferrari, C. Garzoni, A. Riva,
460 G. Snell, F. Sallusto, K. Fink, H.W. Virgin, A. Lanzavecchia, D. Corti, and D. Veesler.
461 2020. Mapping Neutralizing and Immunodominant Sites on the SARS-CoV-2 Spike
462 Receptor-Binding Domain by Structure-Guided High-Resolution Serology. *Cell*
463 Robbiani, D.F., C. Gaebler, F. Muecksch, J.C.C. Lorenzi, Z. Wang, A. Cho, M. Agudelo, C.O.
464 Barnes, A. Gazumyan, S. Finkin, T. Hagglof, T.Y. Oliveira, C. Viant, A. Hurley, H.H.
465 Hoffmann, K.G. Millard, R.G. Kost, M. Cipolla, K. Gordon, F. Bianchini, S.T. Chen, V.

466 Ramos, R. Patel, J. Dizon, I. Shimeliovich, P. Mendoza, H. Hartweger, L. Nogueira, M.
467 Pack, J. Horowitz, F. Schmidt, Y. Weisblum, E. Michailidis, A.W. Ashbrook, E. Waltari,
468 J.E. Pak, K.E. Huey-Tubman, N. Koranda, P.R. Hoffman, A.P. West, Jr., C.M. Rice, T.
469 Hatziioannou, P.J. Bjorkman, P.D. Bieniasz, M. Caskey, and M.C. Nussenzweig. 2020.
470 Convergent antibody responses to SARS-CoV-2 in convalescent individuals. *Nature*
471 Rodda, L.B., J. Netland, L. Shehata, K.B. Pruner, P.M. Morawski, C. Thouvenel, K.K. Takehara,
472 J. Eggenberger, E.A. Hemann, H.R. Waterman, M.L. Fahning, Y. Chen, J. Rathe, C.
473 Stokes, S. Wrenn, B. Fiala, L.P. Carter, J.A. Hamerman, N.P. King, M. Gale, D.J.
474 Campbell, D. Rawlings, and M. Pepper. 2020. Functional SARS-CoV-2-specific immune
475 memory persists after mild COVID-19. *medRxiv*
476 Rydyznski Moderbacher, C., S.I. Ramirez, J.M. Dan, A. Grifoni, K.M. Hastie, D. Weiskopf, S.
477 Belanger, R.K. Abbott, C. Kim, J. Choi, Y. Kato, E.G. Crotty, C. Kim, S.A. Rawlings, J.
478 Mateus, L.P.V. Tse, A. Frazier, R. Baric, B. Peters, J. Greenbaum, E. Ollmann Saphire,
479 D.M. Smith, A. Sette, and S. Crotty. 2020. Antigen-Specific Adaptive Immunity to
480 SARS-CoV-2 in Acute COVID-19 and Associations with Age and Disease Severity. *Cell*
481 Song, G., W.T. He, S. Callaghan, F. Anzanello, D. Huang, J. Ricketts, J.L. Torres, N. Beutler, L.
482 Peng, S. Vargas, J. Cassell, M. Parren, L. Yang, C. Ignacio, D.M. Smith, J.E. Voss, D.
483 Nemazee, A.B. Ward, T. Rogers, D.R. Burton, and R. Andrabi. 2020. Cross-reactive
484 serum and memory B cell responses to spike protein in SARS-CoV-2 and endemic
485 coronavirus infection. *bioRxiv*
486 Staines, H.M., D.E. Kirwan, D.J. Clark, E.R. Adams, Y. Augustin, R.L. Byrne, M. Cocozza, A.I.
487 Cubas-Atienza, L.E. Cuevas, M. Cusinato, B.M.O. Davies, M. Davis, P. Davis, A. Duvoix,
488 N.M. Eckersley, D. Forton, A. Fraser, G. Garrod, L. Hadcocks, Q. Hu, M. Johnson, G.A.
489 Kay, K. Klekotko, Z. Lewis, J. Mensah-Kane, S. Menzies, I. Monahan, C. Moore, G.
490 Nebe-von-Caron, S.I. Owen, C. Sainter, A.A. Sall, J. Schouten, C. Williams, J. Wilkins, K.
491 Woolston, J.R.A. Fitchett, S. Krishna, and T. Planche. 2020. Dynamics of IgG
492 seroconversion and pathophysiology of COVID-19 infections. *medRxiv*
493 Sterlin, D., A. Mathian, M. Miyara, A. Mohr, F. Anna, L. Claer, P. Quentric, J. Fadlallah, P.
494 Ghillani, C. Gunn, R. Hockett, S. Mudumba, A. Guihot, C.-E. Luyt, J. Mayaux, A.
495 Beurton, S. Fourati, J.-M. Lacorte, H. Yssel, C. Parizot, K. Dorgham, P. Charneau, Z.
496 Amoura, and G. Gorochov. 2020. IgA dominates the early neutralizing antibody
497 response to SARS-CoV-2. *medRxiv*
498 Vincent, J.L., R. Moreno, J. Takala, S. Willatts, A. De Mendonça, H. Bruining, C.K. Reinhart,
499 P.M. Suter, and L.G. Thijs. 1996. The SOFA (Sepsis-related Organ Failure Assessment)
500 score to describe organ dysfunction/failure. On behalf of the Working Group on
501 Sepsis-Related Problems of the European Society of Intensive Care Medicine.
502 *Intensive Care Med* 22:707-710.
503 Walls, A.C., Y.J. Park, M.A. Tortorici, A. Wall, A.T. McGuire, and D. Veesler. 2020. Structure,
504 Function, and Antigenicity of the SARS-CoV-2 Spike Glycoprotein. *Cell* 181:281-292
505 e286.
506 Wrapp, D., N. Wang, K.S. Corbett, J.A. Goldsmith, C.L. Hsieh, O. Abiona, B.S. Graham, and J.S.
507 McLellan. 2020. Cryo-EM structure of the 2019-nCoV spike in the prefusion
508 conformation. *Science* 367:1260-1263.
509 Zaki, N., H. Alashwal, and S. Ibrahim. 2020. Association of hypertension, diabetes, stroke,
510 cancer, kidney disease, and high-cholesterol with COVID-19 disease severity and
511 fatality: A systematic review. *Diabetes Metab Syndr* 14:1133-1142.

512 Zhao, J., Q. Yuan, H. Wang, W. Liu, X. Liao, Y. Su, X. Wang, J. Yuan, T. Li, J. Li, S. Qian, C. Hong,
513 F. Wang, Y. Liu, Z. Wang, Q. He, Z. Li, B. He, T. Zhang, Y. Fu, S. Ge, L. Liu, J. Zhang, N.
514 Xia, and Z. Zhang. 2020. Antibody Responses to SARS-CoV-2 in Patients With Novel
515 Coronavirus Disease 2019. *Clin Infect Dis* 71:2027-2034.
516 Zielinski, C.E., D. Corti, F. Mele, D. Pinto, A. Lanzavecchia, and F. Sallusto. 2011. Dissecting
517 the human immunologic memory for pathogens. *Immunol Rev* 240:40-51.
518
519
520 **Figure legends**
521
522 **Figure 1. Study and sampling overview. A)** Overview of study cohort and controls, timeline
523 of longitudinal sampling, the anatomical compartments analyzed, and the measurements
524 performed. AS=asymptomatic. **(B)** Patient sampling overview with first study sample (color)
525 and first convalescent sample (open) indicated for each patient, hospital
526 admission/discharge, level of care and outcome. Patients are group based on peak disease
527 severity (PDS); mild (PDS 1 and 2), moderate (PDS 3 and 4), severe (PDS 5 and 6) and fatal
528 (PDS 7). Individual inclusion sample for each patient is color-coded based on disease severity
529 at the time of sampling.
530
531 **Figure 2. Plasma IgG and IgA responses to N, S and RBD across COVID-19 severity during**
532 **acute disease and convalescence. A)** Individual levels of plasma IgG and IgA (from left to
533 right) in SARS-CoV-2 infected individuals with different peak disease severity (PDS). Data in
534 cyan and green refer to mild disease (PDS 1 and 2), yellow and orange refer to moderate
535 disease (PDS 3 and 4), red and cayenne refer to severe disease (PDS 5 and 6) and grey refers
536 to patients with fatal outcome (PDS 7). Black lines indicate medians and dotted lines indicate
537 the average background level from pre-pandemic healthy controls. Mann-Whitney U was
538 used to compare the groups and considered statistically significant at $p<0.05$. ** $p<0.01$, ***
539 $p<0.001$, **** $p<0.0001$. **B)** Spearman correlation for plasma IgG (top) and IgA (bottom)
540 against the RBD versus days from onset of symptoms during the acute and the convalescent
541 phases are shown. Circles with black lining refer to convalescent samples. **C-D)** Longitudinal
542 measurements of plasma IgG against RBD on a subset of patients with moderate/severe
543 disease and fatal outcome who had low (< 1.0 OD) antibody titers at the time of study
544 inclusion and were longitudinal samples from symptomatic (acute) disease were available.
545 Levels are shown at the time of study inclusion, during the late acute phase and at
546 convalescence, and shown with respect to days from onset of symptoms and as a group
547 comparison. The black lines connect data points from the same individuals. Wilcoxon test
548 was used to compare the groups separately and considered statistically significant at $p<0.05$.
549 **** $p<0.0001$.
550
551 **Figure 3. Airway IgG and IgA responses to RBD across COVID-19 severity during acute**
552 **disease and convalescence. A)** Levels of IgG and IgA to RBD in nostrils swabs (NSW) and
553 nasopharyngeal aspirates (NPA). The black lines indicate median values. Mann-Whitney U
554 was used to compare the group and considered statistically significant at $p<0.05$. *$p<0.05$ **
555 $p<0.01$, *** $p<0.001$, **** $p<0.0001$. **B)** Heat map generated grouping patients according to
556 PDS showing acute and convalescent IgG and IgA titers against N, S and RBD (plasma) and
557 RBC (NSW, NPA and ETA) for each patient. The heat map also includes data from PPHC and
558 PCR-individuals (indicated with PDS 0). Missing data and not available samples are shown in

559 black. **C)** Spearman correlation for NPA versus plasma immunoglobulins against the RBD
560 during acute disease. In A) the line overlaps with not detected (ND) for IgG levels. **D)**
561 Comparison of the levels of RBD IgG/A in patient-matched NSW, NPA, endotracheal
562 aspirates (ETA) and plasma collected at the same time point. The black lines connect data
563 points from the same individuals. Wilcoxon test was used to compare the groups separately
564 and considered statistically significant at $p<0.05$. **** $p<0.0001$.
565
566 **Figure 4. Assessment of frequencies of B cells in the respiratory tract and of circulating S-**
567 **specific memory B cells. A)** Representative example with gating strategy for the
568 identification of lymphocytes (identified as negative for CD14/16/123/66) and of total B cells
569 (CD3-CD19+) in respiratory NPA and ETA samples. **B)** Levels of lymphocytes and of total B
570 cells in NPA and ETA in a subset of patients alongside with NPA from healthy controls. Mann-
571 Whitney test was used to compare the groups and considered statistically significant at
572 $p<0.05$. ** $p<0.01$.
573 **C)** Representative examples with gating strategy of SARS-Cov-2 S-specific memory B cells
574 from one pre-pandemic healthy control, convalescent samples from one SARS-CoV-2 PCR-
575 individual and one mild and one moderate/severe COVID-19 patient. Further
576 characterization of S-positive memory B cells on RBD binding and B cell isotype (IgG+ or IgA+
577 assumed to correspond to IgD-IgM-IgG- B cells). **D)** Pie charts show the cumulative
578 proportion of RBD binding and memory B cell isotypes in convalescent samples from mild
579 (n=6) and moderate/severe (n=8) COVID-19 patients. **E)** Frequencies of S-specific memory B
580 cells in matched acute (filled) and convalescent (filled with black lining) PBMCs in relation to
581 days in the subset of individuals analyzed color-coded according to PDS. Dotted lines on
582 indicate the average background staining from PCR- and PPHC. **F)** Levels of circulating Spike+
583 switched memory B cells during acute disease and convalesce in the subset of patients
584 analyzed, as well as PPHC, color-coded according to PDS. Circles with black lining refer to
585 data during the convalescent phase. Black triangles symbolize the PPHC. Differences were
586 assessed using Kruskal -Wallis with Dunn's multiple comparisons test and considered
587 statistically significant at $p<0.05$. ** $p<0.01$.
588
589 **Table 1.** Clinical characterization of the SARS-CoV-2 infected cohort.
590

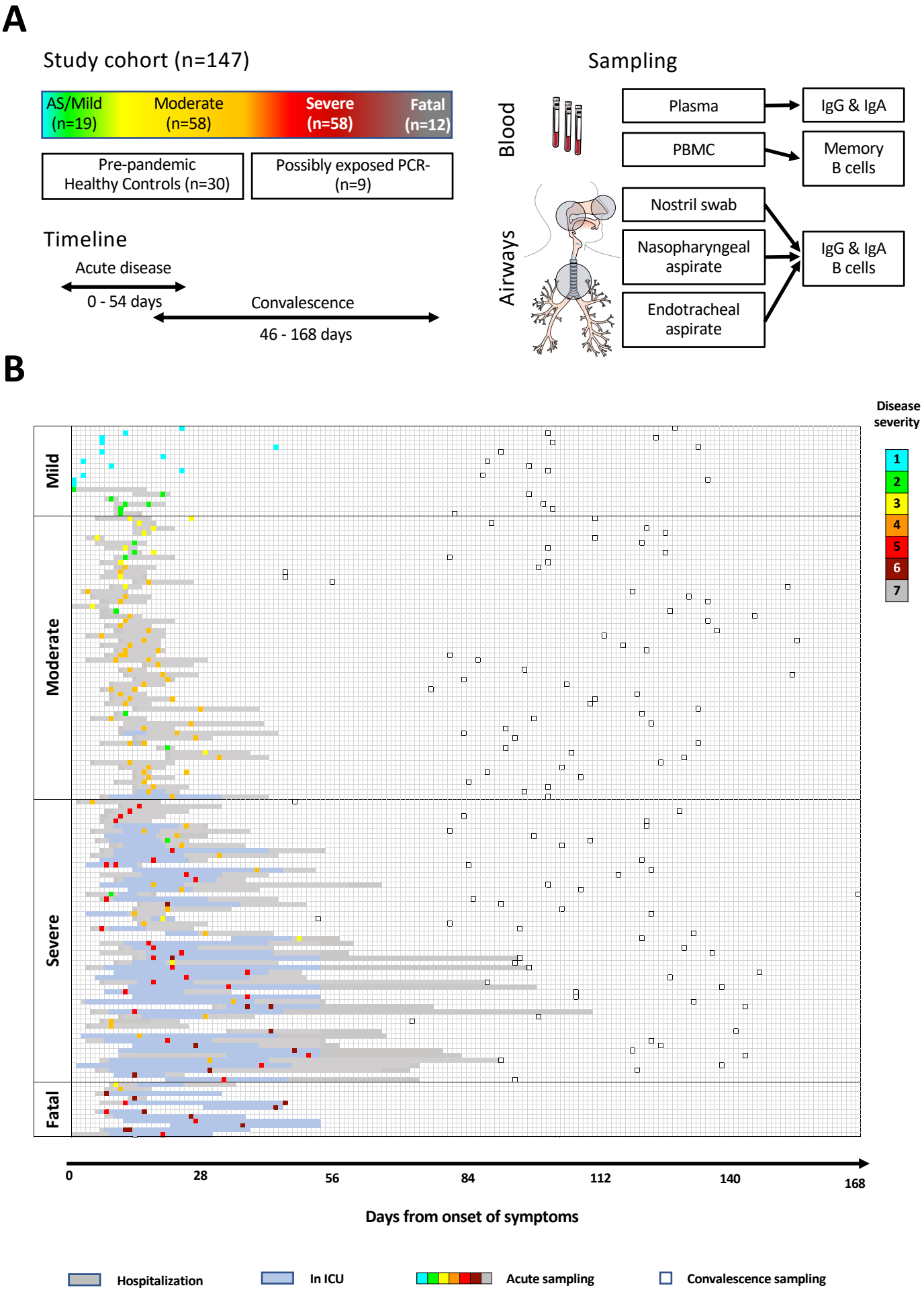
A
Study cohort (n=147)
AS/Mild (n=19)
Moderate (n=58)
Severe (n=58)
Fatal (n=12)
Pre-pandemic Healthy Controls (n=30)
Possibly exposed PCR- (n=9)
Timeline
Acute disease
0 - 54 days
Convalescence
46 - 168 days
Sampling
Blood
Plasma
IgG & IgA
PBMC
Memory B cells
Airways
Nostril swab
Nasopharyngeal aspirate
Endotracheal aspirate
IgG & IgA B cells
B
Disease severity
1
2
3
4
5
6
7
Mild
Moderate
Severe
Fatal
0
28
56
84
112
140
168
Days from onset of symptoms
Hospitalization
In ICU
Acute sampling
Convalescence sampling

Figure 1

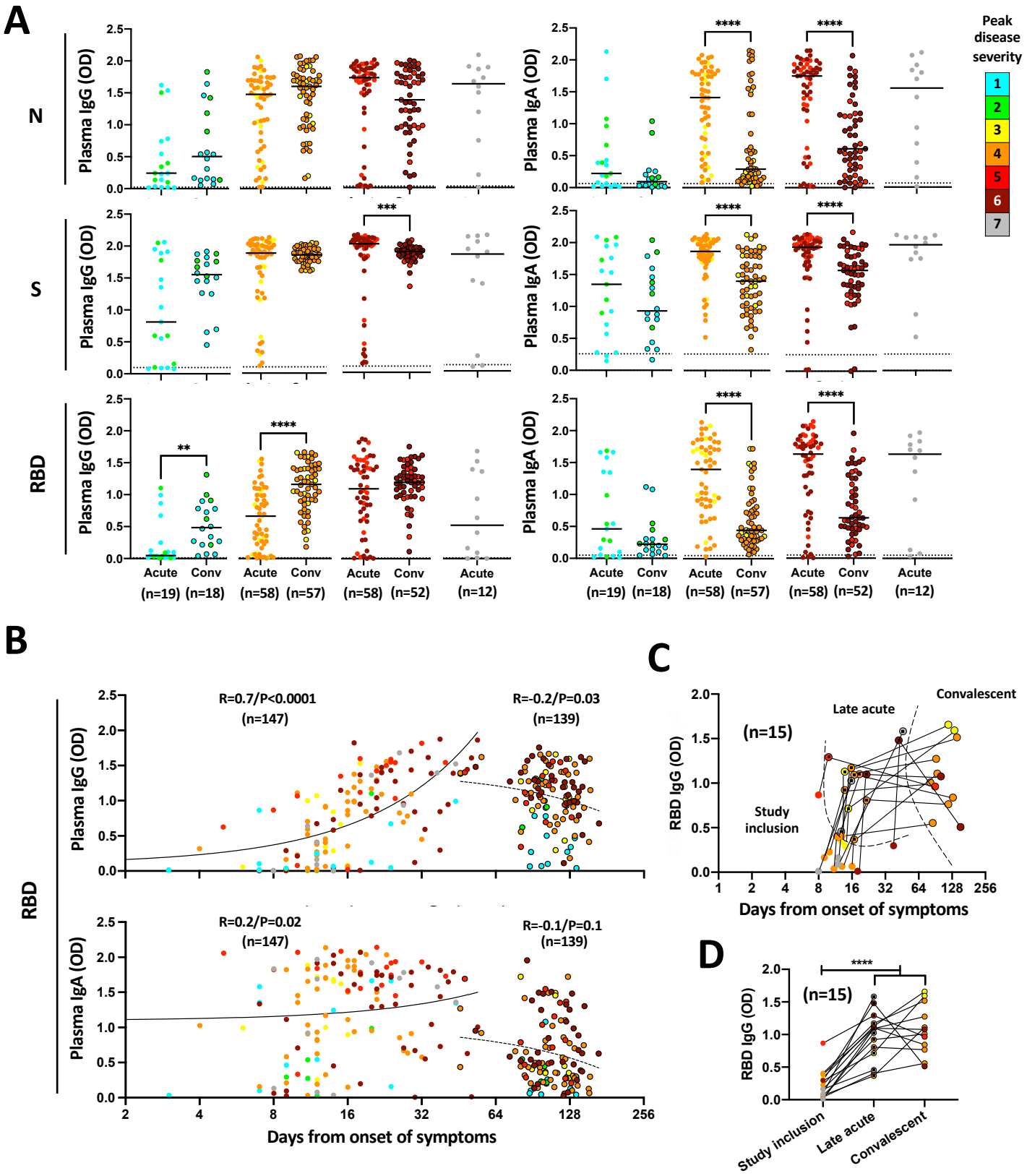
A
N
S
RBD
Plasma IgG (OD)
Plasma IgA (OD)
Peak disease severity
1
2
3
4
5
6
7
Acute (n=19)
Conv (n=18)
Acute (n=58)
Conv (n=57)
Acute (n=58)
Conv (n=52)
Acute (n=12)
B
R=0.7/P<0.0001 (n=147)
R=-0.2/P=0.03 (n=139)
R=0.2/P=0.02 (n=147)
R=-0.1/P=0.1 (n=139)
Days from onset of symptoms
C
(n=15)
Study inclusion
Late acute
Convalescent
RBD IgG (OD)
Days from onset of symptoms
D
(n=15)
RBD IgG (OD)
Study inclusion
Late acute
Convalescent

Figure 2

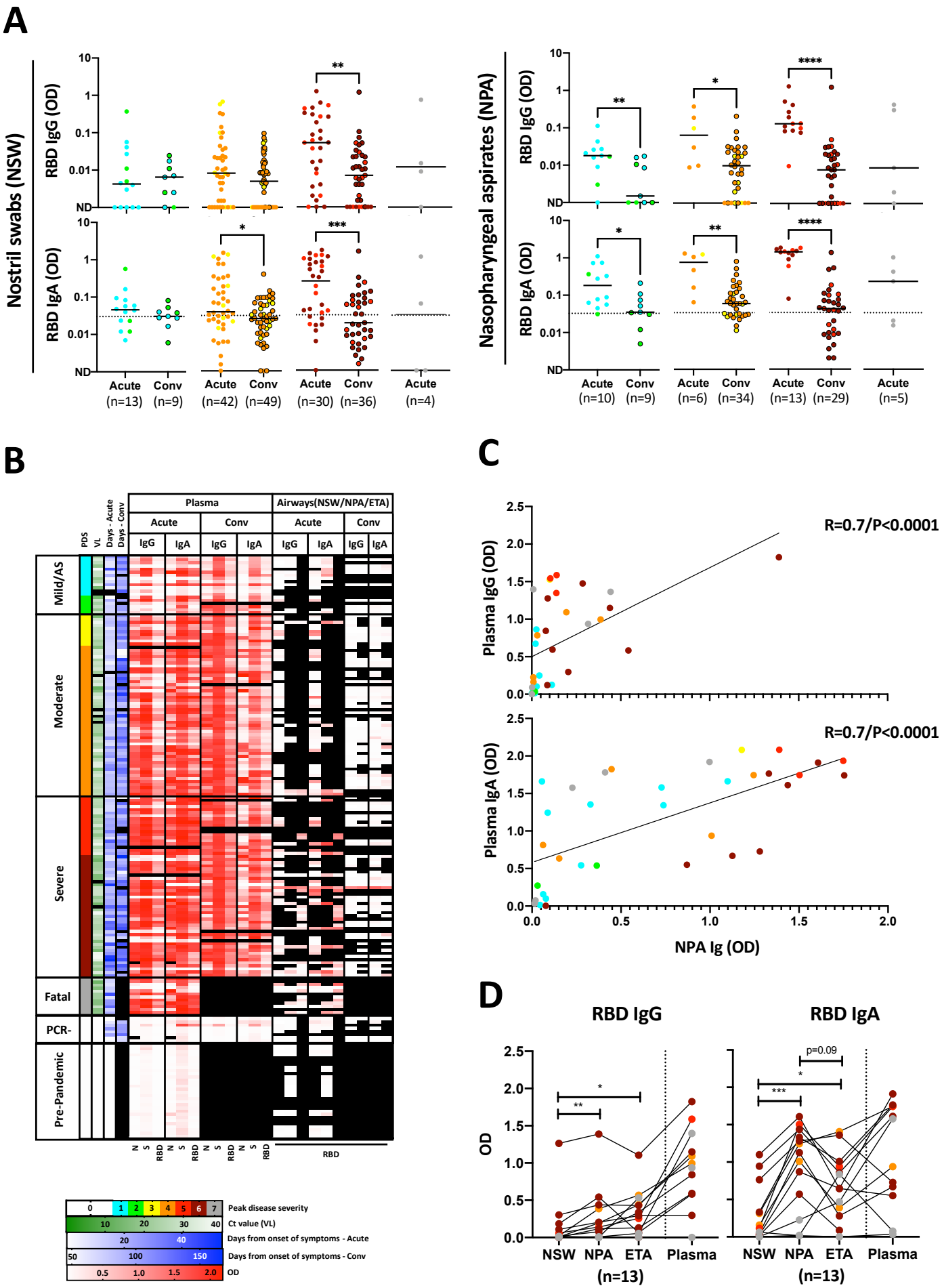
A
Nostril swabs (NSW)
RBD IgG (OD)
RBD IgA (OD)
Nasopharyngeal aspirates (NPA)
Acute (n=13)
Conv (n=9)
Acute (n=42)
Conv (n=49)
Acute (n=30)
Conv (n=36)
Acute (n=4)
Acute (n=10)
Conv (n=9)
Acute (n=6)
Conv (n=34)
Acute (n=13)
Conv (n=29)
Acute (n=5)
B
Plasma
Airways(NSW/NPA/ETA)
Acute
Conv
IgG
IgA
PDS
VL
Days - Acute
Days - Conv
Mild/AS
Moderate
Severe
Fatal
PCR-
Pre-Pandemic
RBD
Peak disease severity
Ct value (VL)
Days from onset of symptoms - Acute
Days from onset of symptoms - Conv
OD
C
R=0.7/P<0.0001
Plasma IgG (OD)
Plasma IgA (OD)
NPA Ig (OD)
D
RBD IgG
RBD IgA
OD
p=0.09
NSW
NPA
ETA
Plasma
(n=13)

Figure 3

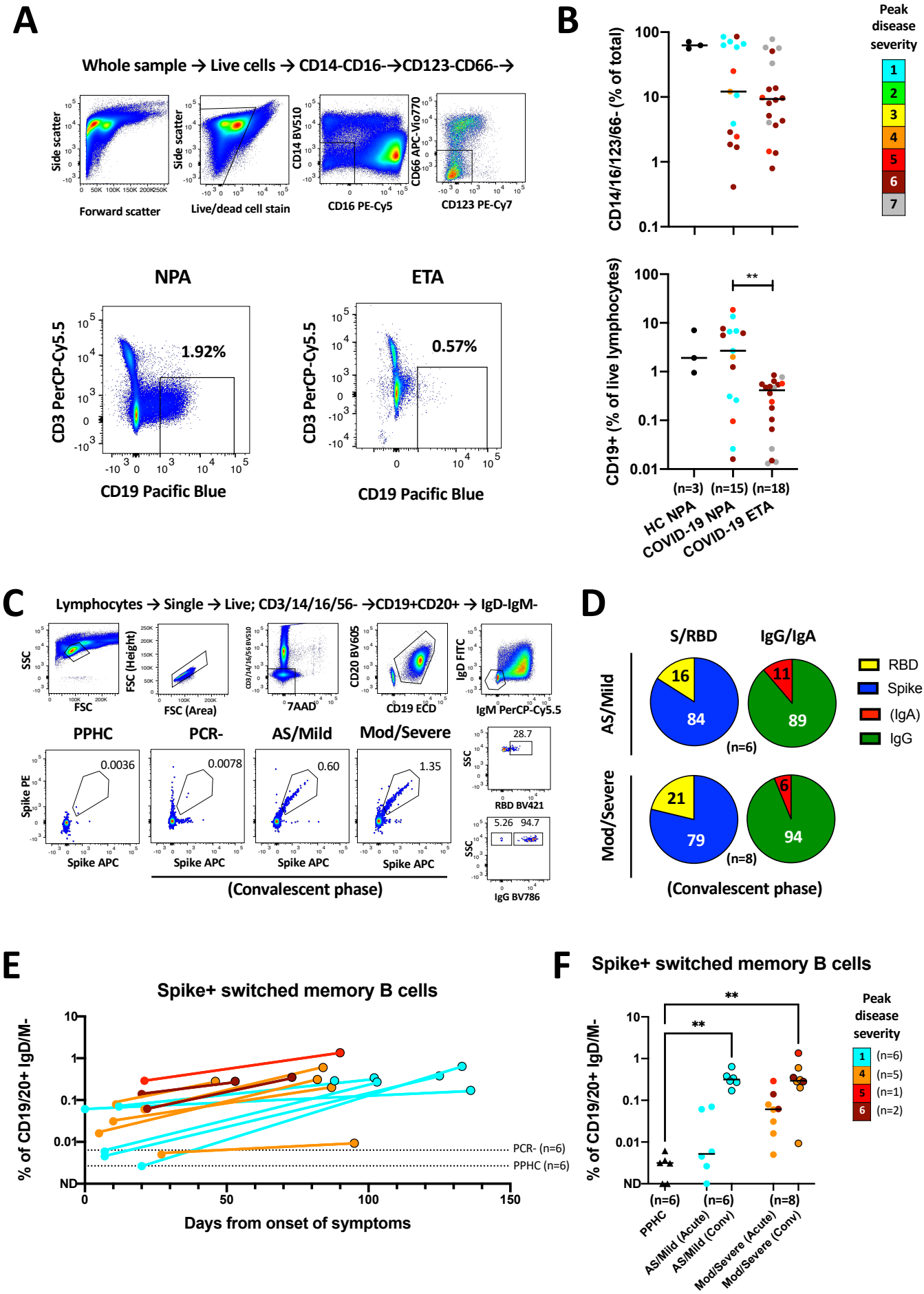
A
Whole sample → Live cells → CD14-CD16-→CD123-CD66-→
Side scatter
Forward scatter
Live/dead cell stain
CD14 BV510
CD16 PE-Cy5
CD66 APC-Vio770
CD123 PE-Cy7
NPA
ETA
CD3 PerCP-Cy5.5
1.92%
0.57%
CD19 Pacific Blue
B
CD14/16/123/66- (% of total)
CD19+ (% of live lymphocytes)
**
(n=3) (n=15) (n=18)
HC NPA
COVID-19 NPA
COVID-19 ETA
Peak disease severity
1
2
3
4
5
6
7
C
Lymphocytes → Single → Live; CD3/14/16/56- →CD19+CD20+ → IgD-IgM-
SSC
FSC
FSC (Height)
FSC (Area)
7AAD
CD20 BV605
CD19 ECD
IgD FITC
IgM PerCP-Cy5.5
PPHC
PCR-
AS/Mild
Mod/Severe
Spike PE
Spike APC
0.0036
0.0078
0.60
1.35
(Convalescent phase)
28.7
RBD BV421
5.26 94.7
IgG BV786
D
S/RBD
IgG/IgA
AS/Mild
Mod/Severe
16
84
11
89
(n=6)
21
79
6
94
(n=8)
(Convalescent phase)
RBD
Spike
(IgA)
IgG
E
Spike+ switched memory B cells
% of CD19/20+ IgD/M-
ND
PCR- (n=6)
PPHC (n=6)
Days from onset of symptoms
F
Spike+ switched memory B cells
**
**
(n=6) (n=6) (n=8)
PPHC
AS/Mild (Acute)
AS/Mild (Conv)
Mod/Severe (Acute)
Mod/Severe (Conv)
Peak disease severity
1 (n=6)
4 (n=5)
5 (n=1)
6 (n=2)

Figure 4

Table 1. Clinical characterization of the SARS-CoV-2 infected cohort.

Disease severity	Mild		Moderate		Severe		Fatal
PDS	1	2	3	4	5*	6*	7
Resp. SOFA score	0	0	1	2	3	4	
Admitted (Y/N)	N	Y	Y	Y	Y	Y	Y
PFI (kPa) SFI	> 53 > 400	> 53 > 400	< 53 ≤ 400	< 40 ≤ 315	< 27 ≤ 235	< 13 < 150	-
Number of individuals (%)	13 (8.8)	6 (4.1)	10 (6.8)	48 (33)	19 (13)	39 (27)	12 (8.2)
Age, mean (Range)	44 (24-72)	60 (41-72)	56 (46-78)	55 (24-76)	57 (42-74)	61 (25-77)	66 (52-78)
Male (%)	5 (38)	2 (33)	6 (60)	38 (79)	15 (79)	34 (87)	9 (75)
Days from symptoms to admission – median (Range)	-	10 (0-14)	8.5 (4-14)	10 (3-21)	7 (2-14)	10 (2-35)	7 (1-28)
Days from symptoms to inclusion “Acute” – median (Range)	9 (3-44)	11 (0-20)	13.5 (6-18)	13 (4-32)	21 (5-40)	22 (7-54)	13 (8-44)
Days from symptoms to follow-up “Conv” – median (Range)	102 (88-136)	99,5 (82-103)	112 (81-127)	109 (46-155)	109 (48-130)	120 (53-168)	-
VL (Ct value) median (Range)	27.5 (40-14)	25.0 (29-14)	26.7 (36-15)	26.8 (36-12)	25.8 (36-19)	24.0 (37-14)	20.5 (32-13)
CCI, mean (SD)	1 (2)	2 (1)	1 (1)	2 (2)	2 (1)	2 (1)	3 (1)
BMI, mean (SD)	24.1 (4.5)	25.1 (2.2)	26.0 (3.2)	30.3 (4.2)	29.2 (5.3)	28.6 (4.7)	28.6 (2.4)
Hypertension (%)	1 (8.3)	0 (0)	2 (20)	20 (42)	8 (42)	15 (38)	9 (75)
Diabetes (%)	2 (17)	0 (0)	1 (10)	14 (29)	5 (26)	9 (23)	3 (25)
Current smokers (%)	0 (0)	0 (0)	2 (20)	5 (11)	1 (5.3)	2 (5.3)	0 (0)
ACE-I (%)	0 (0)	0 (0)	0 (0)	5 (10)	1 (5.3)	4 (10)	1 (9.1)
IS drugs (%)	1 (7.7)	0 (0)	0 (0)	4 (8.3)	2 (11)	5 (13)	1 (8.3)

PDS: Peak Disease Severity
SOFA: Sequential Organ Failure Assessment
PFI: PaO_2/FiO_2-index
SFI: SpO_2/FiO_2-index
VL: Viral Load
CCI: Charlson comorbidity index
BMI: body mass index
ACE-I: angiotensin converting enzyme-inhibitors
IS: immunosuppressive
*Requires mechanical ventilation